

Domain wall conduit behavior in cobalt nanowires grown by focused electron beam induced deposition

A. Fernández-Pacheco, J. M. De Teresa, R. Córdoba, M. R. Ibarra, D. Petit et al.

Citation: *Appl. Phys. Lett.* **94**, 192509 (2009); doi: 10.1063/1.3139068

View online: <http://dx.doi.org/10.1063/1.3139068>

View Table of Contents: <http://apl.aip.org/resource/1/APPLAB/v94/i19>

Published by the American Institute of Physics.

Related Articles

Modeling plastic deformation effect on magnetization in ferromagnetic materials
J. Appl. Phys. **111**, 063909 (2012)

Micromagnetic analysis of switching and domain structure in amorphous metallic nanowires
Appl. Phys. Lett. **100**, 122404 (2012)

Microstructure dependence of Barkhausen voltage pulse width in steel
J. Appl. Phys. **111**, 063903 (2012)

Characterization of domain wall-based traps for magnetic beads separation
J. Appl. Phys. **111**, 07B336 (2012)

Current-driven domain wall motion in heterostructured ferromagnetic nanowires
Appl. Phys. Lett. **100**, 112401 (2012)

Additional information on *Appl. Phys. Lett.*

Journal Homepage: <http://apl.aip.org/>

Journal Information: http://apl.aip.org/about/about_the_journal

Top downloads: http://apl.aip.org/features/most_downloaded

Information for Authors: <http://apl.aip.org/authors>

ADVERTISEMENT



ACCELERATE AMBER AND NAMD BY 5X.
TRY IT ON A FREE, REMOTELY-HOSTED CLUSTER.

[LEARN MORE](#)

Domain wall conduit behavior in cobalt nanowires grown by focused electron beam induced deposition

A. Fernández-Pacheco,^{1,2,3} J. M. De Teresa,^{2,3,a)} R. Córdoba,^{1,3} M. R. Ibarra,^{1,2,3}
D. Petit,^{4,b)} D. E. Read,⁴ L. O'Brien,⁴ E. R. Lewis,⁴ H. T. Zeng,⁴ and R. P. Cowburn⁴

¹Instituto de Nanociencia de Aragón, Universidad de Zaragoza, Zaragoza 50009, Spain

²Instituto de Ciencia de Materiales de Aragón, Universidad de Zaragoza-CSIC, Facultad de Ciencias, Zaragoza 50009, Spain

³Departamento de Física de la Materia Condensada, Universidad de Zaragoza, Zaragoza 50009, Spain

⁴Department of Physics, Nanoscale Magnetics Group, Blackett Laboratory, Imperial College London, Prince Consort Road, London SW7 2BW, United Kingdom

(Received 14 November 2008; accepted 28 April 2009; published online 15 May 2009)

The domain wall nucleation and propagation fields in cobalt nanowires grown by focused electron beam induced deposition are measured using spatially resolved magneto-optical Kerr effect. The study was systematically done for wire widths from 600 to 150 nm, finding significant differences in the value of both fields for the wires, indicating high quality domain wall conduit behavior. The extreme simplicity and flexibility of this technique with respect to the multistep lithographic processes used nowadays opens a different route to create magnetic nanostructures with a good control of the domain wall motion. © 2009 American Institute of Physics.

[DOI: 10.1063/1.3139068]

The local deposition of materials by means of focused-electron-beam-induced-deposition (FEBID) and focused-ion-beam-induced-deposition (FIBID) is an interesting way to grow nanostructures. The beam decomposes the adsorbed molecules as it is scanned on the surface, inducing a localized deposit. Thus, the creation of patterns with nanometer resolution is performed in a direct way, just as “a pencil writing on a paper.” This simplicity is the main advantage with respect to other more well-established lithographic techniques, where several steps, usually involving resist, are required. FEBID and FIBID are currently used in a wide range of research applications, as well as in industry, with carbon and tungsten being the most common used materials.^{1,2} Regarding the deposition of magnetic nanostructures by these techniques, results in the literature can be found for iron³ and cobalt.^{4–7} As the deposits are usually formed from an organometallic precursor, the metal content ranges from a few to several tens of atomic percent but rarely exceeds 50 at. %. The remaining part is mainly composed of carbon, whose fraction becomes a key parameter, which normally alters dramatically the properties of the deposited material.^{1,2,6–8} Thus, the magnetic characterization of these materials is an essential issue. To date, studies of the magnetism of single nanodeposits have been carried out, either in an indirect way, by electrical magnetotransport measurements,^{6,8} or by local probes, such as magnetic force microscopy^{6,8} or electron holography.³ Recently, we have reported extremely highly pure cobalt FEBID deposits, with a saturation magnetization, M_s , of 1330 ± 20 emu/cm³ (around the 95% of the value for pure cobalt) as inferred from magnetotransport characterization.⁹ The local heating induced by the electron irradiation, together with the relatively low temperature for decomposition for this gas precursor, ~100 °C, seems to play a major role for a higher purity in comparison with

other precursors, as has been previously pointed out.^{1,2,7} In our case, this effect is more significant than in previous reports, by the use of a field-emission gun electron column, resulting in Co atomic percentages higher than 90%.

Here we measure magnetic hysteresis loops in single nanometer-sized Co nanowires (NWs) fabricated by FEBID by means of spatially resolved magneto-optical Kerr effect (MOKE) at room temperature. The work is centered on studying the domain wall (DW) conduit properties of such nanostructures,¹⁰ i.e., the possibility to displace DWs at much lower magnetic fields than are needed to nucleate new domains. Controlling the switching of nanometer sized elements is the subject of intense research due to their potential applications in fields such as spintronic logic¹⁰ or DW based memory devices.^{11–13} Most of the work to date in this field has been done on Permalloy NWs. We show in this letter that FEBID-Co is a good alternative for such applications.

L-shaped NWs were grown in a commercial dual beam system (Nova Nanolab by FEI) with an electron beam energy of 10 kV, and a beam current of 2.1 nA, using dicobalt octacarbonyl [Co₂(CO)₈] as the precursor material. A 200 nm wide structure is shown in Fig. 1(a). The time taken to fabricate this structure under the chosen conditions is approximately 2 min. Atomic force microscopy (AFM) measurements were done to measure the exact dimensions of each NW. The thickness of the NWs is 50 nm, with widths (w) between 600 and 150 nm. AFM scans along different zones of the NW were done [see dashed lines in Fig. 1(a)], indicating that a good uniformity in the shape of the structures is attained, with deviations in the section of the wires smaller than 10%. As an example, different scans along a 590-nm-wide wire are shown in Fig. 1(b). Both ends of the NW are pointed to avoid domain nucleation.^{10,13}

Each structure was analyzed using a high sensitivity MOKE magnetometer.¹⁴ The ~5 μm diameter focused laser spot was placed on the horizontal arm of the wire [see circle in Fig. 1(a)]. The component of the magnetization along the

^{a)}Electronic mail: detersa@unizar.es.

^{b)}Electronic mail: d.petit@imperial.ac.uk.

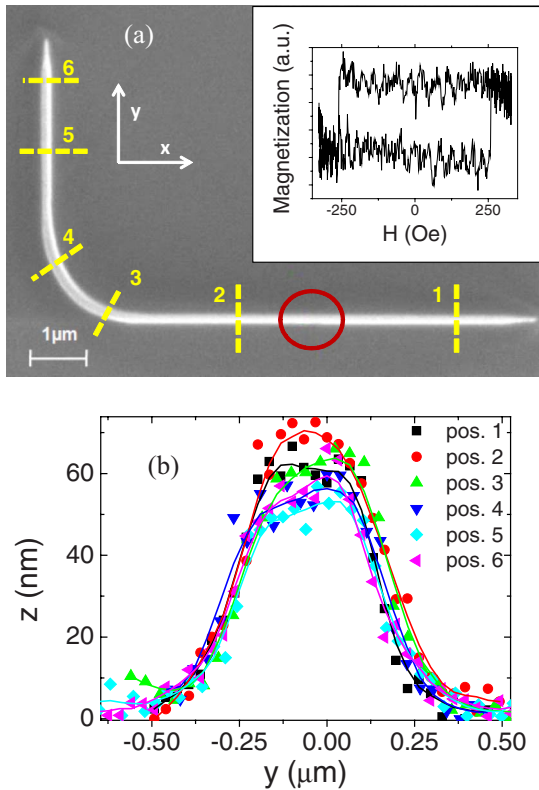


FIG. 1. (Color online) (a) SEM image of a 200-nm-wide L-shaped cobalt NW. The circle represents the MOKE laser spot (not to scale). The dashed lines indicate the AFM profile scans done in different parts of the L-shaped NW. The inset shows a hysteresis loop of this NW obtained from a single-shot measurement. (b) Profile of a 590-nm-wide wire, measured by AFM in different parts of the structure and showing a good uniformity. The numbers associated to the different scan positions are indicated in (a). Lines are guides to the eye.

x axis was determined by measuring the longitudinal Kerr effect. A typical hysteresis loop is shown in the inset of Fig. 1(a), corresponding to a single-sweep experiment. This MOKE setup has demonstrated a high sensitivity for Permalloy, around 10^{-12} emu (Ref. 13). The signal to noise ratio is also very good in these experiments on Co NWs, allowing the clear observation of magnetic switching even in single-shot measurements.

Magnetization measurements along the direction perpendicular to the main axis of the NW (not shown here) revealed that saturation is not reached with the maximum field applied, of 400 Oe. This is in agreement with previous magnetoresistance measurements,⁹ where fields up to 10 kOe were necessary to align the magnetization in the transverse direction. We therefore confirm that the magnetization is completely aligned along the wire axis in the remanent state as a consequence of the shape anisotropy. The binary states can be associated to the two directions of the magnetization ($+M_s, -M_s$) along the easy axis.

To study the possible good control of DWs of the FEBID Co, a quadrupole electromagnet was used to apply two types of (H_x, H_y) magnetic field sequences at a frequency of 1 Hz.¹⁵ In the first procedure, a DW is initially formed at the corner of the NW. In this case, magnetization reversal occurs by the propagation of this DW in the NW. In the second field sequence, no DW is formed at the corner, so the nucleation of a DW is required to reverse the magnetization. A schematic of the processes occurring in the L-shaped structure in

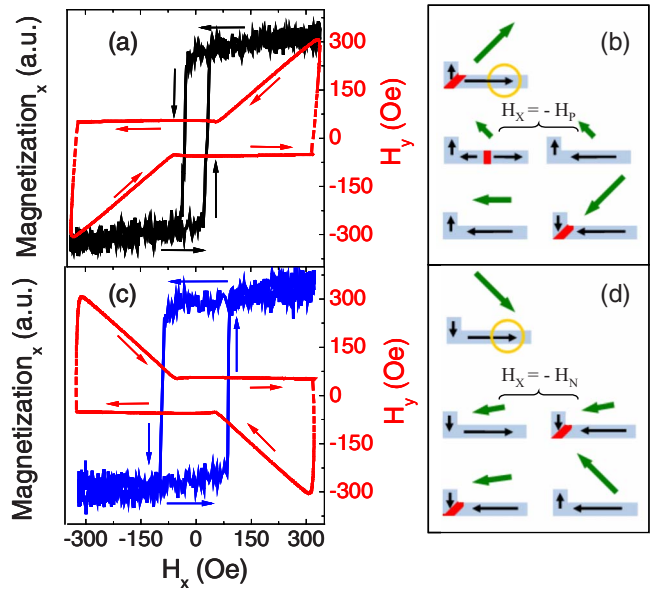


FIG. 2. (Color online) Left: MOKE determined magnetization hysteresis loops (solid lines) and corresponding field sequences (dashed lines) used to measure the propagation (a) and the nucleation field (c) for a 500-nm-wide NW. The arrows on the graphs indicate the sense of variation of the magnetization and the field as the routine is applied. Right: Schematic diagrams of magnetization configurations obtained during half a field cycle (the other half cycle is identical, but with all fields reversed). External arrows show the applied magnetic field; internal arrows show the direction of magnetization in the nanostructure. The circle (not to scale) represents the MOKE laser spot. In (b) (propagation) the magnetic field generates a DW at the corner of the L-shaped NW. As H_x changes to negative values, this DW is propagated through the horizontal arm, switching its magnetization at $-H_p$. The subsequent change of H_y from positive to negative values again induces the generation of a DW in the corner. In (d) (nucleation), the external field saturates the magnetization along the NW. As H_x is reversed to negative values, a reversed domain is nucleated when $H_x = -H_N$; the magnetization in the horizontal arm switches and a DW is now present at the corner of the NW. The change of H_y to positive values again saturates the magnetization along the NW, in the opposite direction to the initial configuration.

half a cycle (from positive to negative magnetic fields) is shown in Figs. 2(b) and 2(d) for the two types of measurements. The other half of the cycle is symmetric. Hysteresis loops for the particular case $w=500$ nm are shown in Fig. 2. To reduce the noise, 30 loops were averaged. In Fig. 2(a), the DW initially formed at the corner is propagated through the horizontal NW, switching its magnetization when the so-called propagation field value ($H_p=30$ Oe) is reached. On the contrary, in Fig. 2(c) no DW is previously created at the corner. The reversal in this case happens at significant higher magnetic fields (at the nucleation field $H_N=91$ Oe). H_p and H_N are very different, with $H_p < H_N$. This behavior is fundamental for possible applications of this material to devices which rely on the formation and control of DWs. It must be noticed that a small field offset in the *y*-direction was maintained in both sequences after the initialization of the magnetization, ensuring that the DW remains in the bottom of the structure and does not propagate in the *y*-direction.¹⁶ This offset (H_y^{off}) was chosen so that $H_y^{off} > H_p$ for the wider NWs, and was maintained when measuring all the NWs for consistency. Systematic measurements of H_p and H_n as a function of H_y show that this transverse offset has very little effect on the switching fields: a maximum variation of 15% was observed in H_p for a 150 nm wire when H_y varied between 20 and 80 Oe. The error bars on Fig. 3 take into account this small effect.

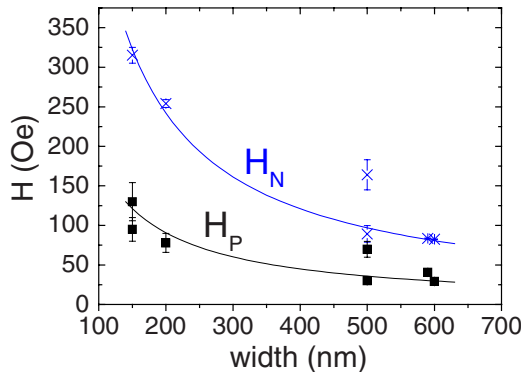


FIG. 3. (Color online) Propagation (H_P) and nucleation fields (H_N) as a function of the NW width. The error bars for the fields take into account the effect of the small H_y -offset used in the field sequences (see text for details).

In Fig. 3, the propagation and nucleation fields are shown as a function of the NW width. In the case of H_N , an inverse relationship with the width is found: $H_N \propto w^{-1}$. This dependence has been previously found by means of magnetoresistance measurements in Co NWs created by electron beam lithography.¹⁷ It can be understood in magnetostatic terms, as a consequence of the shape dependence of the stray field of the wire.^{17,18} We can see that H_P has a similar dependence on width. A good fit is also obtained with the inverse of w . In the case of the nucleation loops, abrupt transitions are always observed, suggesting that the reversal mechanism is by the nucleation of domains plus propagation, starting from a monodomain state.¹⁷ In the case of DW propagation, the transition is not as abrupt as in nucleation field measurements, especially for the narrow NWs. This widening could be thought to be caused by a series of pinning sites under the MOKE spot. However, single-shot loops (not shown here) are all sharp, indicating this is not the case. Therefore, the relatively wider transitions for H_P are caused by the statistical averaging of abrupt switches occurring at close but slightly different fields. These results show that for the dimensions chosen, the conduction of DWs in FEBID Co NWs is excellent. The propagation fields are of a few tens of oersted for the wider NWs. These values are comparable with those ones obtained for thin and narrow Permalloy NWs used nowadays by the scientific community in the area.^{10–15} This is not the case for these narrower NWs, where H_P are too high for most practical magnetoelectronic applications. Thinner NWs should be studied to determine if good DW control is achieved for narrow FEBID Co NWs in a practical range of fields.

In summary, we report direct hysteresis loop measurements performed by MOKE on single Co NWs fabricated by FEBID. We have demonstrated well-controlled formation and motion of DWs in cobalt NWs grown by this technique. In the range of dimensions studied, the shape anisotropy

forces the magnetization to lie in the longitudinal direction of the NW. The process for reversal of the NW is well controlled by the magnetic fields applied, being possible to select either DW propagation, or nucleation of a new domain. Both kinds of processes occur at well-defined fields. Significant differences are found for the fields necessary to reverse the magnetization, if a DW is initially present, or not, in the nanostructure. This demonstrates the conduit properties of the Co FEBID NWs. The implementation of complex magnetic NW networks, necessary for real applications based on DW control, is a routine task with this technique, with the enormous advantage of the simplicity with respect to others with nanometer resolution, and the possibility to create these devices, in principle, on any surface.

This work was supported by the Spanish Ministry of Science (through projects MAT2008-03636-E and MAT2008-06567-C02, including FEDER funding) and by the Aragon Regional Government.

- ¹I. Utke, P. Hoffmann, and J. Melngailis, *J. Vac. Sci. Technol. B* **26**, 1197 (2008).
- ²W. F. van Dorp and C. W. Hagen, *J. Appl. Phys.* **104**, 081301 (2008).
- ³M. Takeuchi, M. Shimojo, R. Che, and K. Furuya, *J. Mater. Sci.* **41**, 2627 (2006).
- ⁴A. Lapicki, E. Ahmad, and T. Suzuki, *J. Magn. Magn. Mater.* **240**, 47 (2002).
- ⁵I. Utke, P. Hoffmann, R. Berger, and L. Scandella, *Appl. Phys. Lett.* **80**, 4792 (2002).
- ⁶G. Boero, I. Utke, T. Bret, N. Quack, M. Todorova, S. Mouaziz, P. Kejik, J. Brugger, R. S. Popovic, and P. Hoffmann, *Appl. Phys. Lett.* **86**, 042503 (2005).
- ⁷I. Utke, J. Michler, P. Gasser, C. Santschi, D. Laub, M. Cantoni, P. A. Buffat, C. Jiao, and P. Hoffmann, *Adv. Eng. Mater.* **7**, 323 (2005).
- ⁸Y. M. Lau, P. C. Chee, J. T. L. Thong, and V. Ng, *J. Vac. Sci. Technol. A* **20**, 1295 (2002).
- ⁹A. Fernández-Pacheco, J. M. De Teresa, R. Córdoba, and M. R. Ibarra, *J. Phys. D* **42**, 055005 (2009).
- ¹⁰D. A. Allwood, G. Xiong, C. C. Faulkner, D. Atkinson, D. Petit, and R. P. Cowburn, *Science* **309**, 1688 (2005).
- ¹¹S. S. P. Parkin, U.S. Patent No. 6,834,005 (16 December 2004); U.S. Patent No. 6,898,132 (16 December 2004); U.S. Patent No. 6,920,062 (14 April 2005); U.S. Patent No. 7,031,178 (5 May 2005); U.S. Patent No. 7,236,386 (8 June 2006).
- ¹²J. Nickel and M. K. Bhattacharyya, U.S. Patent No. 7,078,244 (18 July 2006).
- ¹³D. Atkinson, D. S. Eastwood, and L. K. Bogart, *Appl. Phys. Lett.* **92**, 022510 (2008).
- ¹⁴D. A. Allwood, G. Xiong, M. D. Cooke, and R. P. Cowburn, *J. Phys. D* **36**, 2175 (2003).
- ¹⁵D. Petit, A.-V. Jausovec, D. E. Read, and R. P. Cowburn, *J. Appl. Phys.* **103**, 114307 (2008).
- ¹⁶D. Petit, A.-V. Jausovec, H. T. Zeng, E. Lewis, L. O'Brien, D. E. Read, and R. P. Cowburn, *Appl. Phys. Lett.* **93**, 163108 (2008).
- ¹⁷M. Brands, R. Wieser, C. Hassel, D. Hinzke, and G. Dumpich, *Phys. Rev. B* **74**, 174411 (2006).
- ¹⁸S. Y. Yuan, H. N. Bertram, J. F. Smyth, and S. Schultz, *IEEE Trans. Magn.* **28**, 3171 (1992).